Available online at www.sciencedirect.com
SCIENCE DIRECT®
Applied Catalysis A: General 251 (2003) 435–447
APPLIED CATALYSIS A: GENERAL
www.elsevier.com/locate/apcata

Characterization and performance for propane oxidative dehydrogenation of Li-modified MoO_3/Al_2O_3 catalysts

M.C. Abello [a,*], M.F. Gomez [a], M. Casella [b], O.A. Ferretti [b], M.A. Bañares [c], J.L.G. Fierro [c]

[a] *INTEQUI, Instituto de Investigaciones en Tecnología Química (UNSL-CONICET), Chacabuco y Pedernera, 5700 San Luis, Argentina*
[b] *CINDECA, Centro de Investigación y Desarrollo en Ciencias Aplicadas, Dr. Jorge Ronco (UNLP-CONICET) y Departamento de Ingeniería Química (UNLP), 47 No. 257, 1900 La Plata, Argentina*
[c] *Instituto de Catálisis y Petroleoquímica, CSIC, Cantoblanco, E-28049 Madrid, Spain*

Received 20 February 2003; received in revised form 1 May 2003; accepted 5 May 2003

Abstract

Oxidative dehydrogenation of propane has been studied on Mo/γ-Al_2O_3 catalysts with 13 wt.% of MoO_3 and promoted with Li. The changes induced on catalysts when the support is doped with different amounts of Li (from 0.3 to 1.2 wt.%) have been studied by BET, AAS, XRD, SEM-EDAX, TPR, DRS, XPS, Raman spectroscopy and isopropanol decomposition. The characterization of the samples showed important changes in: texture, Mo supported structure, acid–base properties and reducibility. The Li replaces Brønsted acid sites and decreases the strength of the terminal Mo=O bond. The change in the strength of the terminal Mo=O bond does not correlate with the decrease in Mo species reducibility or with the decrease in propane conversion. This behavior suggests that the terminal Mo=O bond is not the active sites for ODH of propane. The selectivity to propene increases at lower conversion whereas at higher values it leveled off around 25%.

Keywords: Propane oxidative dehydrogenation; Li-doped Mo/γ-Al_2O_3 catalysts; Raman

1. Introduction

In the last decade great interest has been observed in the development of highly selective catalysts for oxidative dehydrogenation (ODH) of light alkanes into alkenes due to their potential application as a source of inexpensive raw materials. A wide variety of catalytic systems has been proposed for this reaction. By far, the most widely studied systems for propane conversion have been around vanadium [1–5] and molybdenum [6–10] based catalysts. In a previous work the influence of Mo loading on γ-Al_2O_3 for the ODH of propane was studied [11]. It was shown that when γ-Al_2O_3 is covered with a molybdate layer below the monolayer values, the catalysts were active but the dehydrogenation selectivity was reduced by the formation of carbon oxides. The results indicated that with Mo loading increasing from 3.6 to 12.7 wt.% propane conversion increased parallel to acidity and to reducibility. At conversions higher than 20% the selectivity to propene leveled off around 25%, irrespective of the molybdenum content.

It is well known that some promoters have an important influence on the catalytic properties for the ODH of alkanes. The modification of the support by alkaline metals and rare earths is probably the most powerful way to adjust catalyst properties and one of

* Corresponding author.
E-mail address: cabello@unsl.edu.ar (M.C. Abello).

0926-860X/$ – see front matter © 2003 Elsevier B.V. All rights reserved.
doi:10.1016/S0926-860X(03)00369-7

the most widely used in practice. They modify not only the redox properties of the system but also the acid–base character of the oxygen species present on the catalyst surface. Most papers on this subject are concerned with potassium additives. The presence of potassium generally decreases the total activity and its effect on selectivities to partial oxidation products can be negative or positive depending on the type of oxidized molecule, the active catalytic component, potassium contents and on the oxidation reaction conditions [12]. Thus, a significant increase in propene selectivity on MgO/γ-Al_2O_3 with the addition of K has been reported in oxidative dehydrogenation of propane [13]. On this catalyst, it was found a parallelism between Mo^{6+} reducibility, surface acidity and catalytic activity. Watson and Ozkan have also noticed a maximum in selectivity and yield of propene by changing the K/Mo molar ratio on silica-titania mixed oxide supported molybdenum catalysts [14]. Chen et al. [15] have reported the effect of alkali (Cs, K, Li) in samples with 4 Mo nm^{-2} surface density on ZrO_2. They found that the presence of alkali/Mo atomic ratio up to 0.2 does not affect the structure of MoO_x domains, but this addition influences the electronic properties and decreases the propane ODH turnover due to the inhibition of secondary propene combustion. Similarly, on alumina-supported vanadia, potassium weakens the terminal V=O bond but does not affect the structure of surface vanadium oxide species [16].

In the present work, the effect of lithium doping on molybdenum supported γ-Al_2O_3 catalysts and on the catalytic activity and selectivity for the ODH of propane has been examined.

2. Experimental

2.1. Sample preparation

Alumina support was calcined at 873 K for 3 h before being used. Different amounts of lithium (0.3, 0.6, 0.9 and 1.2% w/w) were incorporated onto alumina by impregnation with aqueous solution of LiOH. After drying at 373 K overnight and calcination in air at 723 K for 3 h, the doped support was impregnated with an aqueous solution containing ammonium heptamolybdate, AHM, 5×10^{-3} M at pH = 5.6. The volume of AHM was chosen in order to add 13% of MoO_3. After evaporation of the solvent under reduced pressure, the samples were dried at 373 K overnight and further calcined in air at atmospheric pressure according to the following procedure: temperature was raised linearly for 2.5 h up to 723 K, kept constant at 723 K for 3 h, raised linearly up to 873 K, and then, maintained for 5 h at 873 K. Samples were denoted as 13Mo/Al/*x* where *x* indicates the wt.% of Li.

A second type of sample was also prepared to examine the effect of the sequence of lithium introduction. In this sample 0.6 wt.% of lithium was incorporated on the calcined 13Mo/Al/0 catalyst by the impregnation method from a LiOH solution. The solid was again dried and calcined following the same procedure than before. This sample was labeled as Li/13Mo/Al.

2.2. Catalyst characterization

All samples were characterized using the following physicochemical methods:

BET surface area: BET surface areas were measured by using a Micromeritics Accusorb 2100E instrument by adsorption of nitrogen at 77 K on 200 mg of sample previously degassed at 473 K under high vacuum atmosphere for 2 h.

Chemical composition: Molybdenum and lithium contents were determined by atomic absorption spectroscopy. Alkali fusion with $KHSO_4$ and subsequent dissolution with diluted HCl solution brought the samples into solution. The measurements were carried out by standard addition solution method by using a Varian AA275 equipment.

X-ray diffraction (*XRD*): XR diffraction patterns were obtained with a RIGAKU diffractometer operated at 30 kV and 20 mA by using Ni-filtered Cu Kα radiation (λ = 0.15418 nm). The powdered samples were analyzed without previous treatment after deposition on a quartz sample holder. The identification of crystalline phases was made by matching with the JCPDS files.

Diffuse reflectance spectroscopy (*DRS*): UV-Vis spectra were recorded with a Varian Super Scan 3 spectrophotometer equipped with a reflectance attachment. AHM and sodium molybdate were used as reference compounds. Spectra were recorded in the 200–600 nm range under ambient conditions; thus, the samples were hydrated.

X-ray photoelectron spectroscopy (*XPS*): The XP spectra were recorded with a Fisons ESCALAB MK11 200 R spectrometer equipped with a Mg Kα X-ray excitation source ($h\nu = 1253.6$ eV) operated at 12 kV and 10 mA and a hemispherical electron analyzer. Each spectral region was scanned a number of times in order to obtain good signal-to-noise ratios. The residual pressure inside the analysis chamber was kept at values below 7×10^{-9} Torr. Mo 3d, Al 2p, Li 1s, O 1s and C 1s spectra were recorded for each catalyst. All binding energies (BE) were referred to Al 2p line at 74.5 eV.

Raman spectroscopy: The Raman spectra were run with a single-monochromator Renishaw System 1000 equipped with a cooled CCD detector (200 K) and a holographic super-Notch filter. The holographic Notch filter removes the elastic scattering while the Raman signal remains higher than when triple monochromator spectrometers are used. The samples were excited with the 514 nm Ar line, the spectral resolution was better than 3 cm^{-1} and the spectra acquisition consisted of five accumulations of 60 s for each sample. The spectra were acquired under dehydrated conditions at 473 K.

Acid–base properties: Decomposition of isopropanol, IPA, was also used for determining the acid–base properties of the samples. The reaction was carried out between 433 and 473 K in a fixed-bed continuous flow reactor under atmospheric pressure and in the absence of oxygen. The feed consisted of 4.5% IPA and the balance helium. The weight of catalyst was ca. 0.5 g and the flow rate was 40 ml STP min^{-1}. The data for rate calculations were taken after the stationary state was reached and the conversion of isopropanol was less than 15%. Product analysis was performed by gas chromatography using a Carbowax 20 M on Chromosorb W column and a thermal conductivity detector.

Temperature-programmed reduction (*TPR*): Studies were performed in a conventional TPR equipment. This apparatus consists of a gas handling system with mass flow controllers (Matheson), a tubular reactor, a linear temperature programmer (Omega, model CN 2010), a PC for data retrieval, a furnace and various cold traps. In each experiment the sample size was ca. 100 μmol of Mo to assure a good resolution in the experimental conditions used. Before each run, the samples were oxidized in a 30 ml min^{-1} flow of 20 vol.% O_2 in He at 723 K for 30 min. After that, helium was admitted to remove oxygen and then the system cooled at 323 K. The samples were subsequently contacted with a 30 ml min^{-1} flow of 10 vol.% H_2 in Ar and heated, at a rate of 10 K min^{-1}, from 323 K to a final temperature of 985 K and held at 985 K for 2 h. Hydrogen consumption was monitored by a thermal conductivity detector after removing the water formed. Each spectrum was performed twice and the reproducibility was verified. The detector was previously calibrated with pure Ar and the H_2/Ar reduction gas.

SEM-EDAX: Scanning electron micrographs were obtained in a Philips SEM 505 microscope operating at 25 kV and magnification values of 2000–10 000. This instrument is equipped with an energy dispersive X-ray microanalyzer, EDAX 9100, which permits analytical electron microscopy measurements. The samples were sputter coated with gold.

2.3. Catalytic test

The catalysts (0.5–0.85 mm particle diameter) were tested in a fixed-bed quartz tubular reactor operated at atmospheric pressure in the 723–823 K range. The reactor was encased in a furnace, connected to a programmable temperature controller. The reaction temperature was measured with a coaxial thermocouple. The feed was a mixture of 4 vol.% propane, 4 vol.% oxygen and the balance helium. The flow rates of gas streams were controlled by mass flowmeters. The flow rate was 100 ml min^{-1} at room temperature. The reactants and reaction products were alternately analyzed on-line by a Shimadzu GC9A gas chromatograph, equipped with a thermal conductivity detector. A Porapaq Q (80–100 mesh) column was used to separate hydrocarbons and CO_2 and a 1.8 m Carbosphere (80–100 mesh) column for carbon monoxide, methane and oxygen were used. Four analyses were performed at each temperature. The catalyst weight was 0.7 g in all cases. The homogeneous contribution was tested with the empty reactor and no activity was recorded below 853 K. The presence of quartz particles afforded very similar results. The conversion and selectivity to products were evaluated for the exit stream [6,11].

3. Results

In Table 1, the BET specific surface areas and chemical composition of the catalysts are shown. From

Table 1
Nomenclature and characteristics of Li-free and Li-loaded Mo/γ-Al_2O_3 catalysts

Sample	S_{BET} (m^2/g)	%MoO_3	%Li
γ-Al_2O_3	185	0	0
γ-Al_2O_3 + 0.6% Li	177	0	0.58
γ-Al_2O_3 + 1.2% Li	170	0	1.1
13Mo/Al/0	166	12.7	0
13Mo/Al/0.3	122	12.9	0.32
13Mo/Al/0.6	110	12.9	0.55
13Mo/Al/0.9	100	12.8	nd
13Mo/Al/1.2	78	12.7	1.1
Li/13Mo/Al	90	12.4	0.52

nd: not determined.

these results a slight effect in the specific surface areas was observed by doping γ-Al_2O_3 with Li. However, a considerable diminution in the specific surface area of the catalysts was found. Thus, at the 1.2% Li level of doping the specific surface area was reduced to half of its original value, in agreement with literature [17].

The X-ray diffraction patterns of fresh Mo catalysts only showed the presence of peaks characteristic of γ-Al_2O_3 (JCPDS card 10-425), with the only exception of the sample containing 1.2 wt.% Li (Fig. 1). On this sample three undefined lines appear at low angles. They could not be assigned to any lithium compound such as aluminate ($LiAlO_2$, $LiAl_5O_8$), molybdates oxides or carbonate and they do not correspond to $Al_2(MoO_4)_3$ either. One of them already appears in the molybdenum-free 1.2 wt.% Li-doped alumina support and could be ascribed to the formation of a Li–Al–O compound.

Scanning electron microscopy was also applied to examine the morphology of catalysts. The fresh sample of Li-free catalyst shows the structure of bare γ-Al_2O_3. EDAX analysis show a molybdenum to

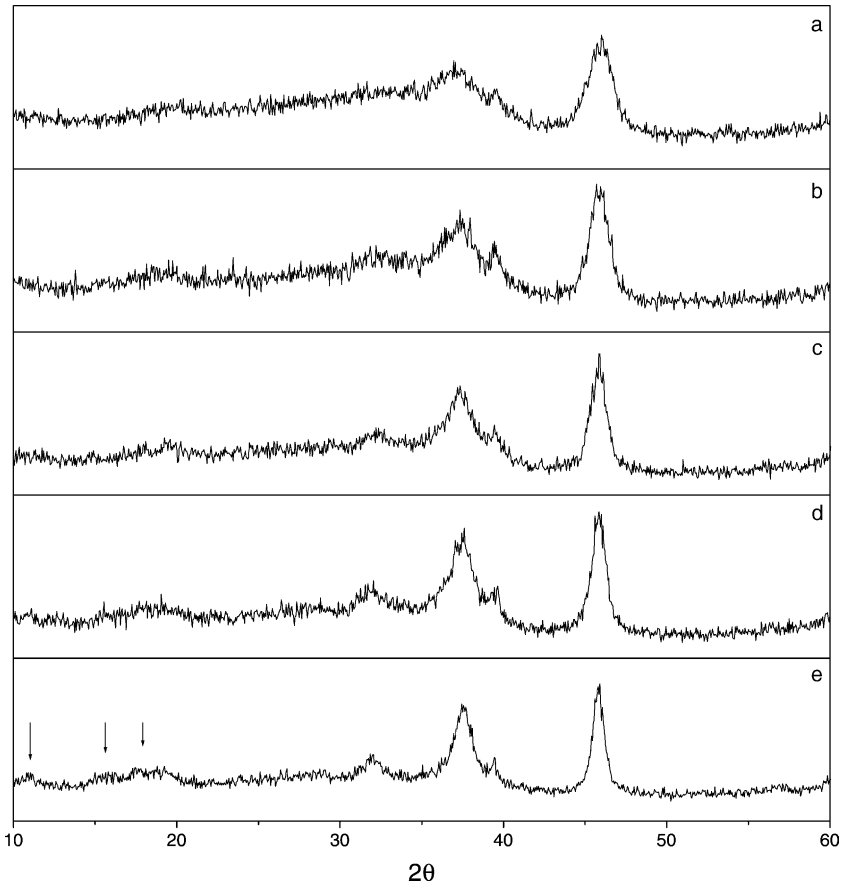

Fig. 1. XRD patterns of Li-loaded alumina-supported Mo oxide catalysts. (a) 0.0; (b) 0.3; (c) 0.6; (d) 0.9; (e) 1.2 wt.% Li.

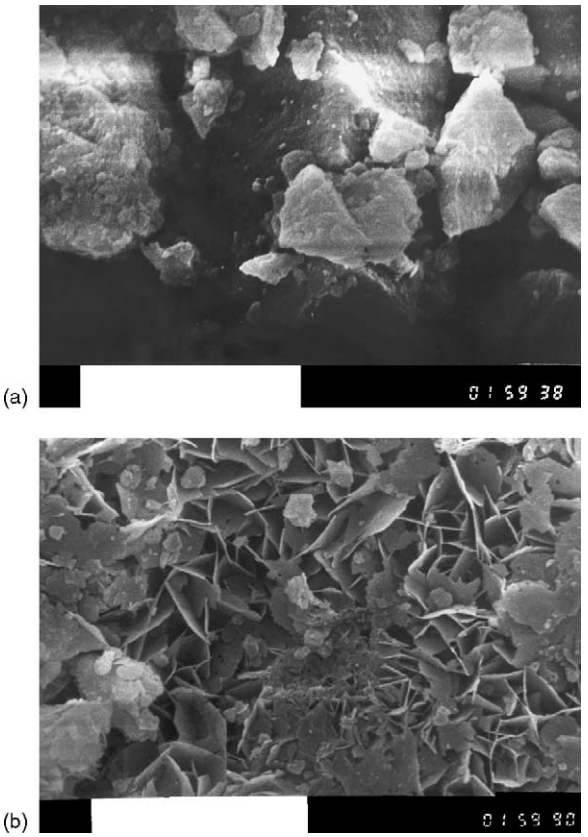

Fig. 2. Scanning electron micrographs of (a) 13Mo/Al/0 and (b) 13Mo/Al/1.2 catalysts. Scale 1 μm.

aluminum signal ratio, which is constant over different areas and corresponds to 15–85% composition. The sample seems to be very homogeneous with highly dispersed Mo oxide species on the support. In the case of Li-loaded samples, the catalyst texture is altered and some "patches" of homogeneous composition (Fig. 2), which agrees satisfactorily with AAS composition are observed. Before Mo impregnation, the modified alumina was calcined at 723 K for 3 h. This temperature corresponds to the fusion temperature of LiOH used as precursor. The melting of Li oxide might account for the change of texture. Similar results were reported by Perrichon and Durupty [18].

UV-Vis diffuse reflectance spectra of hydrated molybdena species are shown in Fig. 3. The spectra of molybdenum(VI) reference compounds in tetrahedral coordination (Na_2MoO_4) and in octahedral coordination ($(NH_4)_6Mo_7O_{24}{\cdot}4H_2O$, AHM) are also included. Tetrahedral molybdenum sodium molybdate exhibits two absorption bands, at 220 and 260 nm, whereas the molybdenum in octahedral coordination presents not only a band around 220 nm, but also additional bands at higher wavelengths (270–290 and 310–350 nm). From literature, it is established that the Mo=O bond of tetrahedral molybdate and Mo–O–Mo bridge bond of the octahedral species exhibit electronic absorptions at 220–250 and 320 nm, respectively [19,20]. The Li-free catalyst shows two absorption bands at 220 and 260 nm and a broad band in the 280–350 nm region suggesting that octahedral species are mainly present [11]. As judging from UV-Vis spectra, the structure of molybdenum species changes substantially in the Li-loaded catalysts. The bands at 220 and at 260 nm are better defined, and that at 360 nm almost disappears. The 1.2 wt.% Li catalyst exhibits a clear decrease in the intensity of the absorption band at higher wavelengths assigned to Mo species in octahedral coordination. This can be understood from the solution chemistry of hydrated molybdena species upon an increase in pH due to increasing amounts of Li [21].

The Raman spectra of dehydrated catalysts in the Ramanshift region 200–1100 cm^{-1} are shown in Fig. 4. The Li-free sample exhibits Raman bands at 1001 and 867 cm^{-1}, which correspond to the stretching mode of terminal Mo=O bond and bridging Mo–O–Mo bonds, respectively. No Raman bands at 817 and 380 cm^{-1}, the most intense of crystalline α-MoO_3 and $Al_2(MoO_4)_3$, respectively, are observed on this sample. This is consistent with the X-ray diffraction results and it suggests that MoO_x species exists as two-dimensional domains. Compared to the spectrum of Li-free sample, some changes were observed upon Li incorporation. The Raman band of polymeric molybdenum species near 867 cm^{-1} decreases with increasing Li content and new bands at 964 and 987 cm^{-1}, which are assigned to lithium molybdates, are also detected. The Raman bands of the stretching mode of the terminal Mo=O bond at 1001 cm^{-1} shifts to lower energies as Li content increases. This is indicative of a weakening of such bond, which becomes longer [22]. Such effect has to be due to some interaction between surface molybdena and surface Li oxide species, which weakens the terminal Mo=O bond.

The acid–base properties of catalysts were compared using the isopropanol test reaction. In Table 2,

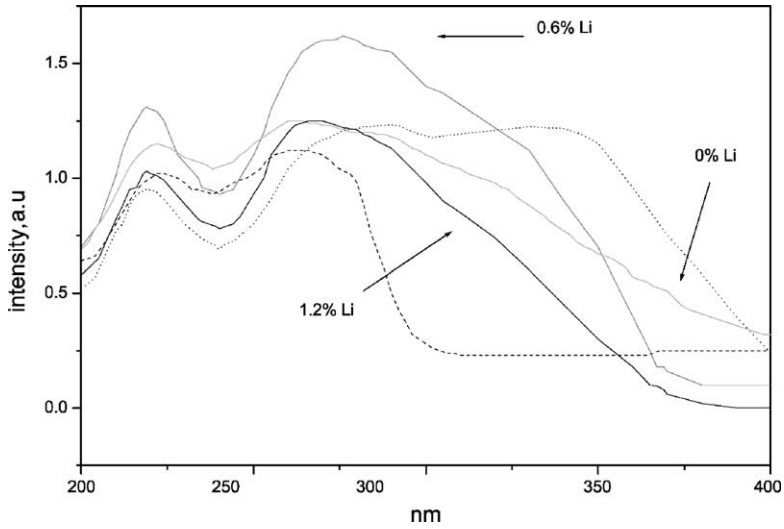

Fig. 3. Diffuse reflectance spectra of Li-loaded alumina-supported Mo oxide catalysts. (- - -) Na_2MoO_4, (· · ·) $(NH_4)_6Mo_7O_{24}$ reference compounds.

the influence of Li loading on dehydration and dehydrogenation rates at 433 K is shown. The dehydration to propene was the main reaction in all cases indicating the predominantly acidic character of the samples. Li shifts the product distribution towards dehydrogenation. The relative rates of dehydration versus dehydrogenation decrease linearly with Li content from ca. 7 to less than 2. When 0.3% of Li is added to the catalyst, dehydrogenation rate to acetone also increases but levels off for the catalysts containing increasing amounts of Li. In any doped samples di-isopropylether formation was observed.

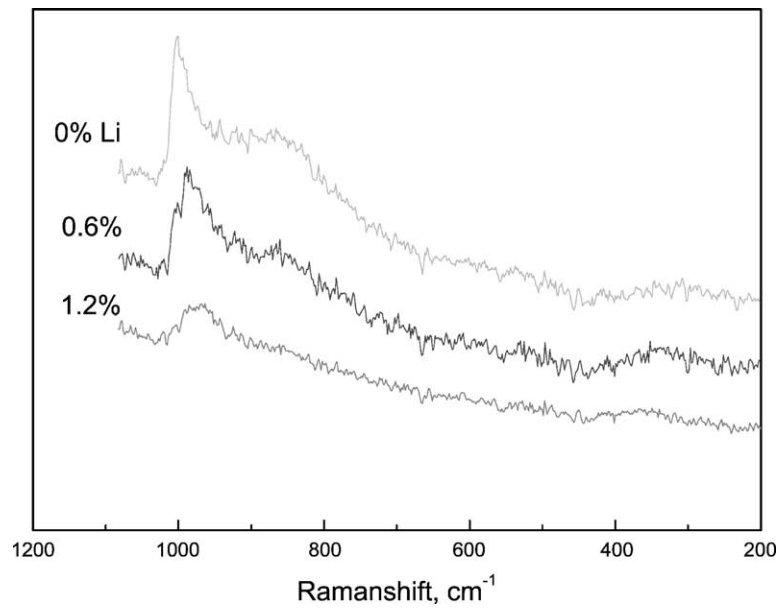

Fig. 4. Raman spectra of fresh Li-loaded Mo/γ-Al_2O_3 catalysts.

Table 2
Isopropanol decomposition on Li-free and Li-loaded Mo/γ-Al_2O_3 catalysts

Sample	$r_{dehydration}$ ($\times 10^8$ mol s^{-1} g^{-1})	$r_{dehydrogenation}$ ($\times 10^8$ mol s^{-1} g^{-1})	Rate ratio, $r_{dehydration}/r_{dehydrogenation}$	Atomic Li/Mo ratio
13Mo/Al/0	19.2	2.7	7.1	0
13Mo/Al/0.3	11.3	3.0	3.8	0.48
13Mo/Al/0.6	8.6	3.0	2.9	0.98
13Mo/Al/0.9	7.2	3.1	2.3	1.47
13Mo/Al/1.2	5.6	3.1	1.8	1.96

The isopropanol decomposition proceeds by two parallel routes: dehydration to propene on acidic (rather weak or moderate) sites and dehydrogenation to acetone on redox (basic) sites. The isopropanol decomposition cannot distinguish between the Brønsted and Lewis sites. Nevertheless, Aramendía et al. [23] have reported that the dehydration activity during isopropanol decomposition could be correlated with Brønsted acidity. Then, it can be inferred that the Brønsted acidity decreases with increasing Li content. Similar results were found by Martin et al. [24] on MoO_3/TiO_2 catalysts.

Table 3 summarizes the values of binding energies of Mo $3d_{5/2}$, O 1s and Li 2s core-levels of the calcined samples. The binding energy of Mo $3d_{5/2}$ level varies in a narrow range 233.2–232.9 eV. This value corresponds to molybdenum, Mo^{6+} ions in an environment of oxide anions and it is in agreement with literature data [25–27]. In Li-loaded catalysts, the binding energies of Mo $3d_{5/2}$ and Li 1s levels slightly decrease. No changes are apparently observed in the binding energies of O 1s core-level. It is also observed that the full width at half maximum (fwhm) is rather large (3.8–4.4 eV), which could be taken as an indication that Li is present in more than one chemical environment. The proportion of Mo and Li atoms, relative to Al atoms, has also been evaluated by photoelectron spectroscopy. It is observed that the Mo/Al atomic ratios are high and always above the bulk ratio (0.051). This observation points to a high dispersion degree of the MoO_3 on the γ-Al_2O_3 surface and decreases upon Li incorporation. This is consistent with the Raman molecular information that evidence the non-existence of aggregates MoO_3 crystal and only the presence of surface molybdenum oxide species. Mo/Al XPS ratio moderately increases when Li content increases from 0.3 to 0.6%, probably due to the coverage of Al sites by Li cations or changes in the texture of the system, with lower BET area.

Catalyst reducibility was examined by temperature-programmed reduction (TPR). The TPR profiles of the fresh samples (Fig. 5) show two well-resolved reduction peaks with some differences in the temperature at the maximum. In all samples the maximum of the first reduction peak appears in the temperature range where the oxydehydrogenation reaction takes place. As illustrated in Table 4, this maximum shifts to higher temperatures upon increasing Li-loading. For Li-free sample, the temperature is 725 K whereas it increases up to 776 K for 0.3% Li-loaded sample. These results suggest that the reducibility of Mo^{6+} decreases. A decrease in the reducibility of supported molybdena

Table 3
Binding Energies for Mo $3d_{5/2}$, O 1s and Li 1s levels and surface atomic ratios of fresh Mo/γ-Al_2O_3 catalysts

Sample	Binding energy (eV)			Mo 3d/Al 2p
	Mo $3d_{5/2}$	O 1s	Li 1s	
13Mo/Al/0	233.2	–	–	0.100
13Mo/Al/0.3	232.9	531.6	55.3	0.070
13Mo/Al/0.6	233.0	531.7	55.2	0.076
13Mo/Al/0.9	232.9	531.7	55.2	0.078
13Mo/Al/1.2	232.9	531.6	54.9	0.077

Table 4
Temperatures at the maximum in TPR profiles and change in average oxidation number during TPR experiments

Sample	T_{max} 1st peak (K)	H_2 consumption (μmoles H_2 per 100 μmol Mo)	ΔON
13Mo/Al/0	725	110.7	2.2
13Mo/Al/0.3	776	108.3	2.2
13Mo/Al/0.6	785	120.7	2.4
13Mo/Al/0.9	792	124.0	2.5
13Mo/Al/1.2	800	116.1	2.3

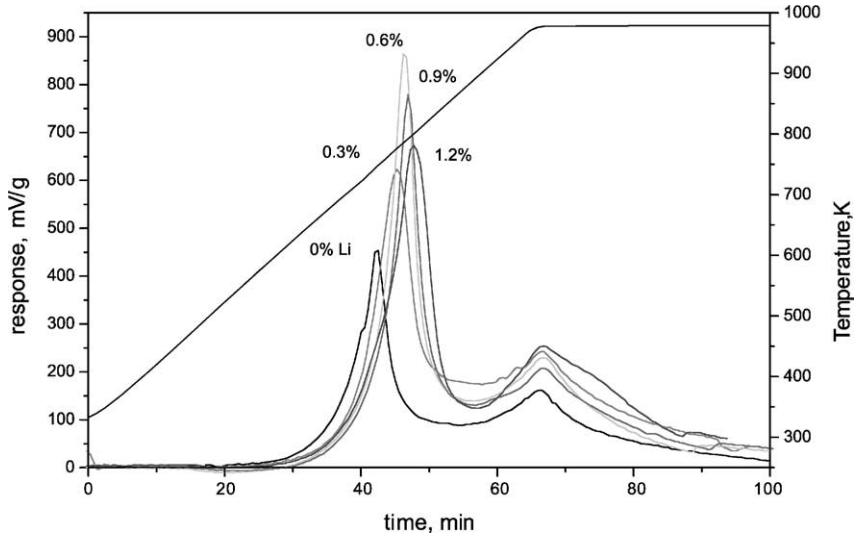

Fig. 5. H_2-TPR profiles of Li-loaded alumina-supported Mo oxide catalysts.

when modified with alkaline metals has been previously reported [28,29]. The changes in temperature are lower as the Li content increases. A similar role of alkali cation loading on supported molybdena is observed for Na doping on silica-supported molybdenum oxide catalysts [28]. Similarly to what is presented in this work, an initial addition of Na does not form new compounds and strongly decrease the reducibility of surface molybdenum oxide species while any further increase of Na loading affords less intense shifts in the TPR profiles [28]. The intensity of the first TPR peak increases upon adding Li up to 0.6 wt.% and then decreases. This behavior would be explained assuming that the structure of molybdenum species changes and some Li-molybdates are developed at higher Li-contents. The sharper reduction profiles would evidence a narrower distribution on the nature of molybdenum oxide species. Lithium retards the reduction of surface molybdenum oxide species. The stabilization of Mo by adding potassium in Mo/Al_2O_3 catalysts has been also reported [25]. The extent of reduction has been characterized by the change in the average oxidation number of Mo, ΔON, which depends on the amount on the reducibility of Mo species and on the experimental conditions of TPR [11]. For example, $\Delta ON = 2$ indicates an average reduction of Mo^{6+} to Mo^{4+}. Table 4 compiles the amount of H_2 uptake and the corresponding ΔON calculated from the whole TPR profiles. No significant changes in the extent of reduction is observed, molybdenum being mainly reduced to Mo^{4+} under our TPR experimental conditions. These results show that Li does not significantly affect the global consumption of H_2 but it increases the reduction resistance of molybdenum species.

Concerning to ODH of propane, the results of conversion (X%), oxygen consumption (R_{O_2}%) and product selectivities are shown in Table 5. Propene and carbon oxides were the main products. Oxygenated products other than carbon oxides were not observed under the experimental conditions used. Ethane was only detected on Li-free samples and on the catalysts with 0.3 and 0.6 wt.% Li at the highest temperature employed and at high conversion levels of propane. This fact is in agreement with the lower acidity of Li-loaded catalysts. It is well known that hydrocarbon cracking is favored on strong acid sites. In Table 5, it is also shown the catalytic results on Li/13Mo/Al catalyst. Its performance is almost the same to that of the 13Mo/Al/0.6 catalyst. Then, it can be suggested that the incorporation sequence of Li does not affect the properties and the molecular structures of surface molybdenum oxide species (at least in this loading level).

The most important effect of the addition of Li are the marked decrease in the catalytic activity (Table 5), the decrease of global reducibility and the weakening

Table 5
Catalytic results in propane oxidation over Li-loaded alumina-supported Mo oxide catalysts

Sample	T (K)	R_{O_2}%	X%	S_{C_3}%	S_{CO_2}%	S_{CO}%	S_{C_2}%	Specific activity[a] × 10^9	TOF[b], (10^{-4} s^{-1})
13Mo/Al/0	723	36.2	13.6	32.4	27.0	40.6	–	2.9	5.45
	773	79.7	28.5	26.6	28.2	44.2	1.0	6.1	11.4
	823	99.9	36.2	25.1	25.7	47.2	2.0	7.7	14.5
13Mo/Al/0.3	723	9.6	5.9	66.1	9.0	24.9	–	1.7	2.32
	773	34.4	16.2	46.1	16.1	37.7	–	4.7	6.39
	823	83.6	32.2	27.9	20.2	49.6	1.4	9.3	12.7
13Mo/Al/0.6	723	5.2	3.8	72.3	9.5	18.2	–	1.2	1.5
	773	23.7	12.1	51.5	14.1	34.4	–	3.9	4.77
	823	65.5	26.4	33.9	20.2	45.1	0.7	8.5	10.4
13Mo/Al/0.9	723	3.3	2.8	79.5	8.7	11.8	–	1.0	1.11
	773	11.4	7.8	69.0	10.9	20.0	–	2.7	3.10
	823	47.2	20.8	42.5	19.0	38.5	–	7.4	8.28
13Mo/Al/1.2	723	2.0	1.9	84.3	9.7	6.0	–	0.9	0.76
	773	8.3	5.9	74.6	15.2	10.2	–	2.7	2.36
	823	32.3	14.9	47.6	20.6	31.8	–	6.7	5.97
Li/13Mo/Al	723	4.3	3.1	72.5	7.8	19.7	–	1.1	1.27
	773	25.5	12.4	51.5	10.9	37.5	–	4.4	5.08
	823	69.8	26.6	35.2	19.4	45.0	0.5	9.5	10.9

[a] Specific activity = $X/(W/F_{C_3})S_{BET}$, $mol_{C_3H_8}$ m^{-2} s^{-1}.
[b] Assuming that all Mo sites are active.

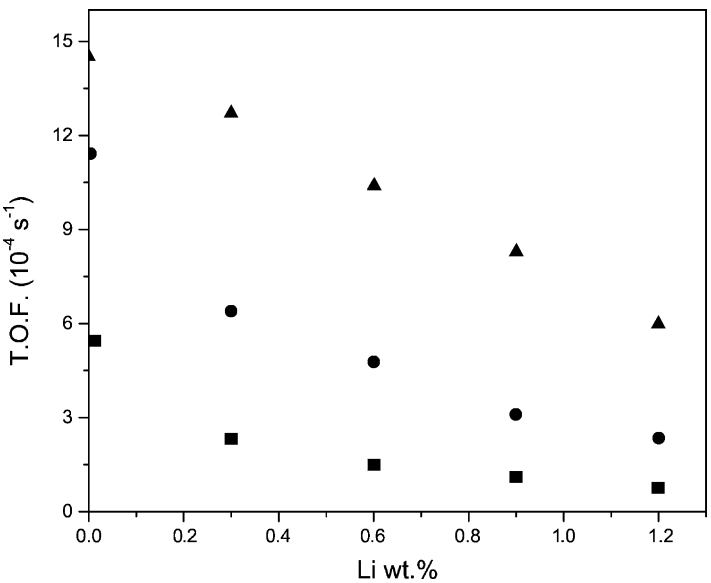

Fig. 6. TOF in ODH of propane at different temperatures. (■) 723 K; (●) 773 K; (▲) 823 K.

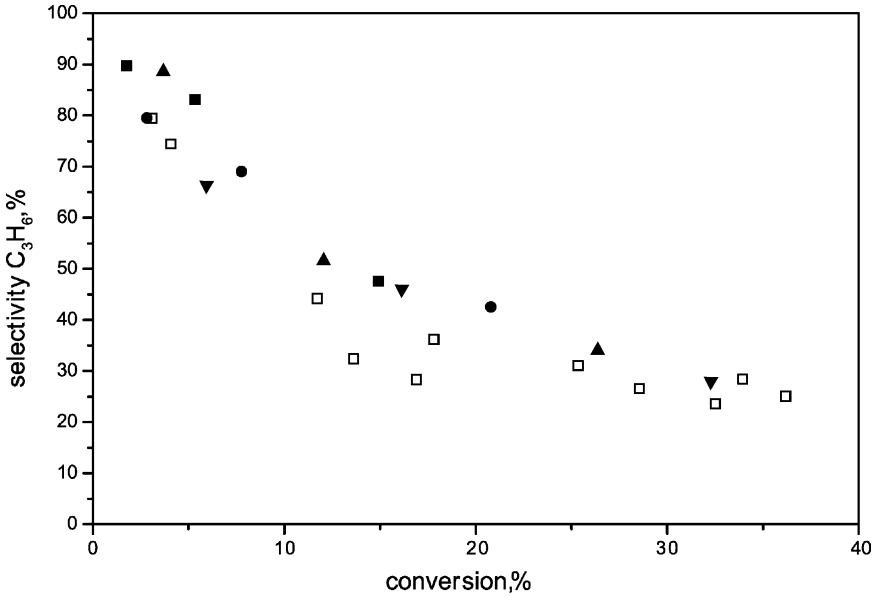

Fig. 7. Variation of propene selectivity with conversion obtained in the ODH of propane. Li-free catalyst, open symbols; Li-loaded catalysts, solid symbols. (▼) 0.3, (▲) 0.6, (●) 0.9, (■) 1.2 wt.% Li.

of the Mo=O bond. It can be observed that the decrease in propane conversion is not due to the decrease in the specific area, because the specific activity per square meter of catalyst shows the same trend (Table 5). The pronounced effect of Li on propane activity is clearly illustrated in Fig. 6 where the turnover frequencies, TOF (catalytic activity expressed as the number of reacted moles of propane per molybdena unit per second assuming that all Mo is active) are presented at different temperatures.

Looking at the effect of temperature on selectivity, it is seen that the selectivity to CO_2 is almost constant on Li-free catalyst (25–28%), whereas it is lower on Li-loaded samples, increasing from 9 to 20% when the reaction temperature increases from 723 to 773 K. The presence of Li replacing Brønsted acid sites would eliminate nonselective route of oxidation on acidic centers decreasing total activity. Such trend is consistent with that observed for K-doped alumina-supported vanadia catalysts [16].

Concerning to the propene selectivity, it can be observed in Fig. 7 that the addition of Li results in an improvement at conversions lower than 20%. At higher conversion levels, the propene selectivity decreases as a result of the marked increase in CO selectivity and levels off at ca. 25%. This effect is independent of reaction temperature (723–823 K) and all points practically fit the same curve.

Based on the data discussed above, it is clear that different kinetic results are due to effects induced by the Li additive on the active and selective centers of the catalyst surface. An apparent activation energy could be estimated from the temperature dependence of conversion, while recognizing the limited significance of the calculated value. The apparent activation energy for propane conversion over 723–823 K range, is rather constant with increasing Li concentration. Since the conversion on Li-free catalyst is underevaluated at 823 K (the oxygen consumption is practically 100% at this condition), the same apparent activation energy could be estimated. This value is around 84–96 kJ mol^{-1} (between 0 and 1.2 wt.% Li). Then, the Li addition affects the number of active sites without changing the reaction mechanism.

4. Discussion

In this study, the ODH of propane has been examined over on Mo/γ-Al_2O_3 catalysts containing a fixed

amount of MoO_3 (13 wt.%) and loaded with different amounts of Li. In all samples Mo species are very well dispersed on alumina surface. The vibrational (Raman) and electronic spectra of calcined samples show that molybdenum mainly exists in an octahedral coordination over the Li-free catalyst, with no observation of an α-MoO_3 phase. Some Li-molybdates may be present over doped catalysts. Lithium can react to form highly dispersed molybdates in different coordination depending on the molar ratio Li/Mo. Thus, Mo^{6+} has tetrahedral unit in Li_2MoO_4, tetrahedral and octahedral units in $Li_2Mo_2O_7$ and octahedral unit in $Li_2Mo_3O_{10}$ and $Li_2Mo_4O_{13}$. The Raman spectra show a decrease in the intensity of Mo polymeric species, a weakening of the terminal Mo=O bond and the appearance of new bands at 964 and 987 cm^{-1} for the sample containing 1.2 wt.% Li, which are ascribed to Li-molybdates. On this sample, an important fraction of Mo could be incorporated in a Li-molybdate matrix, predominantly in tetrahedral coordination (i.e. Li_2MoO_4), which does not contribute to propane activation. Kordulis et al. [17] have also suggested the formation of surface alkali molybdate on alumina at the expense of the supported polymeric Mo^{6+}, as it has been demonstrated for Na, K and Cs doping on molybdena/silica catalysts [28]. The formation of Li_2MoO_4 has also been observed on MoO_3/TiO_2 loaded with 1% of Li [24].

Upon increasing the Li-content on 13Mo/γ-Al_2O_3 base catalyst, the most important effect observed for the ODH of propane is the marked decrease in catalytic activity. Li addition decreases the Brønsted acidity as it can be inferred from the isopropanol decomposition test reaction. The importance of these acid sites associated with polymeric Mo species in the propane activation has been recognized in a previous work [11], so that the strong decrease in activity may be related to replacement of Mo–OH Brønsted acid sites. In addition to affecting the surface acidity, the presence of Li influences the reducibility of molybdenum species. The reducibility, as determined by the temperature at which the maximum hydrogen-consumption occurs, decreases on the Li-loaded catalysts even though molybdenum oxide is reducible in the temperature range where the ODH reaction is carried out. Several studies have proposed that alkane ODH rates increase as active metal oxides become more reducible [30,31]. Both factors clearly affect the activity of catalyst. In Fig. 8, a linear correlation between the reducibility of catalysts measured by the T_{max} of TPR first peak and the propane conversion is evident. The strong relationship between

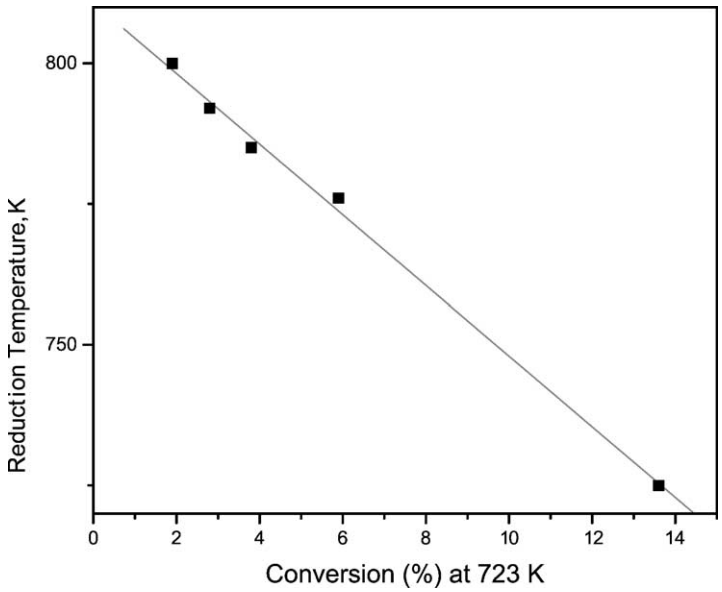

Fig. 8. Evolution of catalyst reducibility vs. propane conversion at 723 K.

these two parameters and the weakening of the Mo=O terminal bond with Li-doping evidenced by Raman spectroscopy suggest that the terminal Mo=O bond is not the active site for ODH of propane. Recently, Chen et al. [32] have found that the C–H bond dissociation of alkane depends sensitively on the ability of the active oxide domains to transfer electrons from lattice oxygen atoms to metal centers more than the tendency of oxides to reduce in H_2. The slight decrease in the binding energy of Mo 3d core levels upon adding Li provides some evidence about changes in the electronic properties of doped catalysts.

Concerning to propene selectivity, Fig. 7 shows an important promotion effect of Li at conversion levels lower than 20% (i.e. selectivity increases from 50 to 60% at conversion of 10%). Such increase can be explained taking into account the lower formation of carbon oxide due to the inhibition effect of Li on the combustion and the lower acidity (which decreases the formation of C2 hydrocarbons and allows the easier desorption of propene). At higher conversions, which correspond to catalysts with Li/Mo < 1, 13Mo/Al/0.3 and 13Mo/Al/0.6, the selectivity levels off at around 25% and the positive effect of Li seems to be lost. The acidity and reducibility of these catalysts are lower than 13Mo/Al/0, however irrelevant changes in selectivities are observed. Nevertheless, these cases are no longer under differential conditions (conversion values below 10%) and comparisons are not accurate.

The trend of CO_2 selectivity with Li loading between 0.3 and 1.2 wt.% strongly suggests that the combustion capacity of Li-containing catalysts is inhibited; thus, decreasing the direct oxidation of propane. Therefore, Li could control the formation of undesired CO_x products and becomes itself an interesting promoter.

5. Conclusions

Oxidative dehydrogenation of propane has been studied on Mo/γ-Al_2O_3 catalysts with 13 wt.% of MoO_3 and promoted with Li. The addition of Li affects the structure and properties of supported molybdenum oxide species. The presence of Li replacing Brønsted acid sites would eliminate nonselective route of oxidation on acidic centers decreasing total activity. The Raman spectra shows a weakening of the Mo=O bond on Li-loaded catalysts. The change in the strength of the terminal Mo=O bond does not correlate with the decrease in Mo species reducibility or with the marked decrease in propane conversion. This behavior suggests that the terminal Mo=O bond is not the active sites for ODH of propane, since this bond becomes more labile upon interaction with lithium. Similar catalytic performance was obtained independently of the sequence of Li addition.

Acknowledgements

The authors wish to thank Dr. Rivarola for helpful discussions. Financial support is acknowledged to CONICET, to Universidad Nacional de San Luis and Universidad Nacional de La Plata. CICYT Grant IN96-0053, Spain, partially funded the acquisition of the Raman spectrometer.

References

[1] E.A. Mamedov, V. Cortes Corberán, Appl. Catal. A: Gen. 127 (1995) 1.
[2] M.A. Chaar, D. Patel, M.C. Kung, H.H. Kung, J. Catal. 105 (1987) 483.
[3] M.A. Chaar, D. Patel, H.H. Kung, J. Catal. 109 (1988) 463.
[4] A. Corma, J.M. Lopez Nieto, N. Paredes, J. Catal. 144 (1993) 425.
[5] J.G. Eon, R. Olier, J.C. Volta, J. Catal. 145 (1994) 318.
[6] L.E. Cadus, M.C. Abello, M.F. Gomez, J.B. Rivarola, I&EC Res. 35 (1996) 14.
[7] M.C. Abello, M.F. Gomez, L.E. Cadus, I&EC Res. 35 (1996) 2137.
[8] L.E. Cadus, M.F. Gomez, M.C. Abello, Catal. Lett. 43 (1997) 229.
[9] C. Mazzocchia, C. Aboumrad, C. Diagne, E. Tempesti, J.M. Herrmann, G. Thomas, Catal. Lett. 10 (1991) 181.
[10] Y.-S. Yoon, N. Fujikawa, W. Ueda, Y. Moro-oka, K.-W. Lee, Catal. Today 24 (1995) 327.
[11] M.C. Abello, M.F. Gomez, O. Ferretti, Appl. Catal. A: Gen. 207 (2001) 421.
[12] R. Grabowski, B. Grzybowska, K. Samson, J. Slocznski, J. Stoch, K. Wcislo, Appl. Catal. A: Gen. 125 (1995) 129.
[13] M.C. Abello, M.F. Gomez, L.E. Cadus, Catal. Lett. 53 (1998) 185.
[14] R.B. Watson, U.S. Ozkan, J. Catal. 191 (2000) 12.
[15] K. Chen, S. Xie, A.T. Bell, E. Iglesia, J. Catal. 195 (2000) 244.
[16] G. Garcia Cortez, J.L.G. Fierro, M.A. Bañares, Catal. Today, in press.

[17] Ch. Kordulis, S. Voliotis, A. Lycourghiotis, D. Vattis, B. Delmon, Appl. Catal. 11 (1984) 179.
[18] V. Perrichon, M.C. Durupty, Appl. Catal. 42 (1988) 217.
[19] F. Delannay, Characterization of Heterogeneous Catalysts, Marcel Dekker, New York, 1984, p. 150.
[20] G. Xiong, C. Li, Z. Feng, P. Ying, Q. Xin, J. Liu, J. Catal. 186 (1999) 234.
[21] H. Hu, I.E. Wachs, S.R. Bare, J. Phys. Chem. 99 (1995) 10897.
[22] F.D. Hardcastle, I.E. Wachs, J. Raman Spectrosc. 27 (1990) 683.
[23] M.A. Aramendía, V. Borau, C. Jimenez, J.M. Marinas, A. Porras, F.J. Urbano, J. Catal. 161 (1996) 829.
[24] C. Martin, I. Martin, V. Rives, P. Malet, J. Catal. 161 (1996) 87.
[25] S. De Canio, M. Cataldo, E. De Canio, D. Storm, J. Catal. 119 (1989) 256.
[26] I. Oliveros, M.J. Perez Zurita, C. Scott, M.R. Goldwasser, J. Goldwasser, S. Rondon, M. Houalla, D.M. Hercules, J. Catal. 171 (1997) 485.
[27] W. Grunert, A. Stakheev, W. Morke, R. Feldhaus, K. Anders, E. Shapiro, K. Minachev, J. Catal. 135 (1992) 269.
[28] M.A. Bañares, N.D. Spencer, M.D. Jones, I.E. Wachs, J. Catal. 146 (1994) 204.
[29] C.L. O'Young, J. Phys. Chem. 93 (1989) 2016.
[30] M.A. Bañares, Catal. Today 51 (1999) 319.
[31] E.N. Voskeresankaya, V.G. Roguleva, A.G. Anshits, Catal. Rev. Sci. Eng. 37 (1995) 101.
[32] K. Chen, A. Bell, E. Iglesia, J. Catal. 209 (2002) 35.